Tracing the Initiation of the Tribeč Mountain Exhumation by Laser-Probe $^{40}Ar/^{39}Ar$ Dating of Seismogenic Pseudotachylytes (Western Carpathians, Slovakia)

Journal Item

Tracing the Initiation of the Tribeč Mountain Exhumation by Laser-Probe $^{40}Ar/^{39}Ar$ Dating of Seismogenic Pseudotachylytes (Western Carpathians, Slovakia)

Milan Kohút[1,*] *and Sarah C. Sherlock*[2]

1. Earth Science Institute, Slovak Academy of Sciences, Dubravska cesta 9, 840 05 Bratislava, Slovakia; 2. Centre for Earth, Planetary, Space and Astronomical Research (CEPSAR), Department of Environment, Earth and Ecosystems, Open University, Milton Keynes MK2 2PE, United Kingdom

ABSTRACT

The seismogenic pseudotachylytes from the Tribeč Mountains (Western Carpathians, Slovakia) were dated by means of the laser microprobe $^{40}Ar/^{39}Ar$ method. The Tribeč Mountain crystalline basement was buried to 5–7.5-km depths, where it experienced approximately >110°C and <210°C thermal conditions. The dated pseudotachylytes have spot ages between 58 ± 1 and 46 ± 1 Ma with a weighted mean age of 49.7 ± 1.3 Ma, indicating that seismic activity caused their origin, the propagation of subvertical basement marginal faults, and/or the inception of basement unroofing processes in the southern part of the Central Carpathian Paleogene Basin. The extensional tectonics were responsible for the exhumation of basement highs and the opening of the intramontane depressions on the northwest margin of the Pannonian Basin.

Introduction

The evolution of relief and topography mirrors the endogenic and exogenic processes that are responsible for the uplift, erosion, and exhumation of rock blocks in mountain belts (e.g., England and Molnar 1990; Ring et al. 1999). Generally, the dynamic interaction of processes controlling deformation of the lithosphere and those operating at its surface can be investigated as exhumation histories of mountains and sedimentary records in neighboring depressions. The spatial coincidence between the location of enhanced erosion, maximum crustal uplift rates, and lowest steepness indices suggests a positive feedback between erosional unloading and tectonic forcing (England and Molnar 1990). Understanding the tectonic evolution of the relief-forming processes depends on our ability to determine the age of tectonic features—for example, ductile shear zones and brittle faults—on a variety of crustal scales. There are a number of isotopic dating methods suitable for dating shear zones that formed under mid- to lower-crustal conditions due to the higher temperatures of mineral formation and consequent isotopic equilibration of the Sm-Nd, U-Pb, and Rb-Sr systems, for example. It is difficult to determine the ages of brittle faults, formed in upper-crustal conditions (≤300°C), and where sedimentary or volcanic markers are absent. If fault movements cause differential vertical movements of crustal blocks that exceed a few hundred meters, it may be possible to determine the age of the fault movement by fission track and (U-Th)/He thermochronology (Wagner and Van den Haute 1992; Reiners and Brandon 2006), but where only minor or strike-slip displacement has taken place there is a paucity of tools for dating such structures. However, where pseudotachylytes occur they may be used to date fault movements. Small melt volumes generated during flash friction connected to the seismic/tectonic events in Earth's upper crust play a significant role in our ability to determine the age of the tectonic processes in orogenic belts and intracratonic areas. Pseudotachylyte (dark aphanitic fault-related rock composed of friction-derived melt material interspersed with refractory clasts and crystals from the host rock) is thought to have formed in response to seismic activity during the collapse phase of meteorite impact craters and rapid tectonic faulting or landslides (e.g., Philpotts 1964; Sibson

Manuscript received May 27, 2015; accepted October 2, 2015; electronically published March 10, 2016.

* Author for correspondence; e-mail: milan626@gmail.com.

[The Journal of Geology, 2016, volume 124, p. 255–265] 0022-1376/2016/12402-0007$15.00. DOI: 10.1086/684443

1975; Magloughlin and Spray 1992; Reimold 1995). The high potassium content of the melt material derived from the host-rock micas and/or amphiboles makes pseudotachylyte an ideal candidate for $^{40}Ar/^{39}Ar$ dating (e.g., Reimold et al. 1990; Sherlock and Hetzel 2001; see also Sherlock et al. 2008, 2009). In this study, $^{40}Ar/^{39}Ar$ laser-probe dating has been applied to pseudotachylytes from the Tribeč Mountains of the Western Carpathians.

The European Alpides (Alps and Carpathians) terminated outward expansion approximately during the Eocene-Miocene interval, and tectonic uplift and exhumation shifted into the orogen interior (e.g., Csontos et al. 1992; Kováč et al 1994; Kováč 2000; Froitzheim et al. 2008; Minár et al. 2011). This transfer is consistent with a change from orogenic construction to orogenic destruction, reflecting an increase in the ratio of erosional flux to accretionary flux. $^{40}Ar/^{39}Ar$ ages of pseudotachylytes from the Tatra Mountains reflect initial basement exhumation of these mountains (Kohút and Sherlock 2003) in the Western Carpathians. Although pseudotachylytes were recently described from another Western Carpathian area—the Tribeč Mountains (Madarás et al. 2004)—their age was unknown. The aim of this article is to present $^{40}Ar/^{39}Ar$ laser microprobe data from these pseudotachylytes and to discuss Eocene-Miocene tectonic activity within the Tribeč Mountains and sediment supply to the surrounding areas—the southern margin of the Central Carpathian Paleogene Basin (CCPB) and the northwestern margin of the Pannonian Basin.

Geological Setting

The Western Carpathians are the northernmost part of the Carpathian orogenic belt, joining the Eastern Alps in the west, continuing eastward to the Eastern Carpathians, and bordered to the north by the European Platform and to the south by the Neogene Pannonian Basin. The Western Carpathians record a complex history that includes Variscan and Alpine orogeny. Three orogen-parallel pre-Alpine principal structural zones form the internal parts of the Western Carpathians (Inner Western Carpathians [IWC]) from the north to the south: the Tatric, the Veporic, and the Gemeric Superunits (fig. 1*a*; Andrusov 1968; Plašienka 1999). These principal superunits comprise Variscan crystalline basement and its sedimentary cover and are defined as thick-skinned crustal sheets that were tectonically juxtaposed through north-directed thrusting in the early Late Cretaceous (Andrusov 1968). Cenozoic evolution of Western Carpathian basement areas is problematic because of a lack of suitable data (Kováč 2000). Recent ideas are based on the work of Kováč et al. (1994), who concluded from geochronological, stratigraphic, and fission track data that internal (southern) parts of Tatric domains were exhumed and cooled to near surface conditions in the course of postorogenic unroofing during early Paleogene times (55–35 Ma), with gradual (35–20 and 20–10 Ma) waning toward the external border to the north. Contrary to this, Kázmér et al. (2003) and Danišík et al. (2004, 2008, 2010, 2011), based on sedimentological, fission track, and thermal modeling data, pointed out that the CCPB forearc basin played a more important role in the geodynamic evolution of the IWC than was previously thought. These authors proposed that during the Eocene period the pre-Cenozoic basement of the IWC underwent maximum burial, when it was loaded by a thick pile of CCPB sediments. While Kováč et al. (1994) favor a progressive exhumation and simple cooling of crystalline complexes migrating from internal parts of the belt toward the orogenic front, Danišík et al. (2004, 2008, 2010, 2011) argued for a complex thermal history with at least one phase of reheating related to a Paleogene sedimentary burial and/or the Miocene mantle upwelling associated with volcanic activity that caused increased heat flow (the Miocene thermal event; Danišík et al. 2008) and gradual Miocene sedimentation.

The Tribeč Mountains represent the western part of the core mountain inner belt of the Tatric Superunit (fig. 1) of the Central Western Carpathians (Andrusov 1968; Plašienka 1999). The Tribeč Mountain crystalline basement comprises pre-Mesozoic metamorphic and granitic rocks overlain by Mesozoic sedimentary cover sequences and nappes. The Tribeč Mountains form an asymmetric horst structure that trends northeast-southwest and dips toward the southeast and is flanked by two Neogene depressions, the Komjatice Depression on the east and the Rišňovce Depression on the west. These two Neogene depressions form the northern margin of the Pannonian (Danube) Basin. The geological structure of the Tribeč Mountains is relatively simple: crystalline basement is predominantly a deeply eroded Variscan granitic pluton that is well exposed in the central core of the range, whereas the Mesozoic cover complexes, locally affected by Alpine metamorphism, are preserved in the marginal parts. The Mesozoic nappe units are sparsely conserved in northeastern and southwestern marginal parts. Borehole RAO-3 was drilled in the central part of the mountains (GPS coordinates: N48°26′52.80″, E18°14′07.52″) in which pseudotachylyte veins were discovered at depths of 108–111 m (Madarás et al. 2004), in medium- to coarse-grained I-type biotite granodiorites and tonalites.

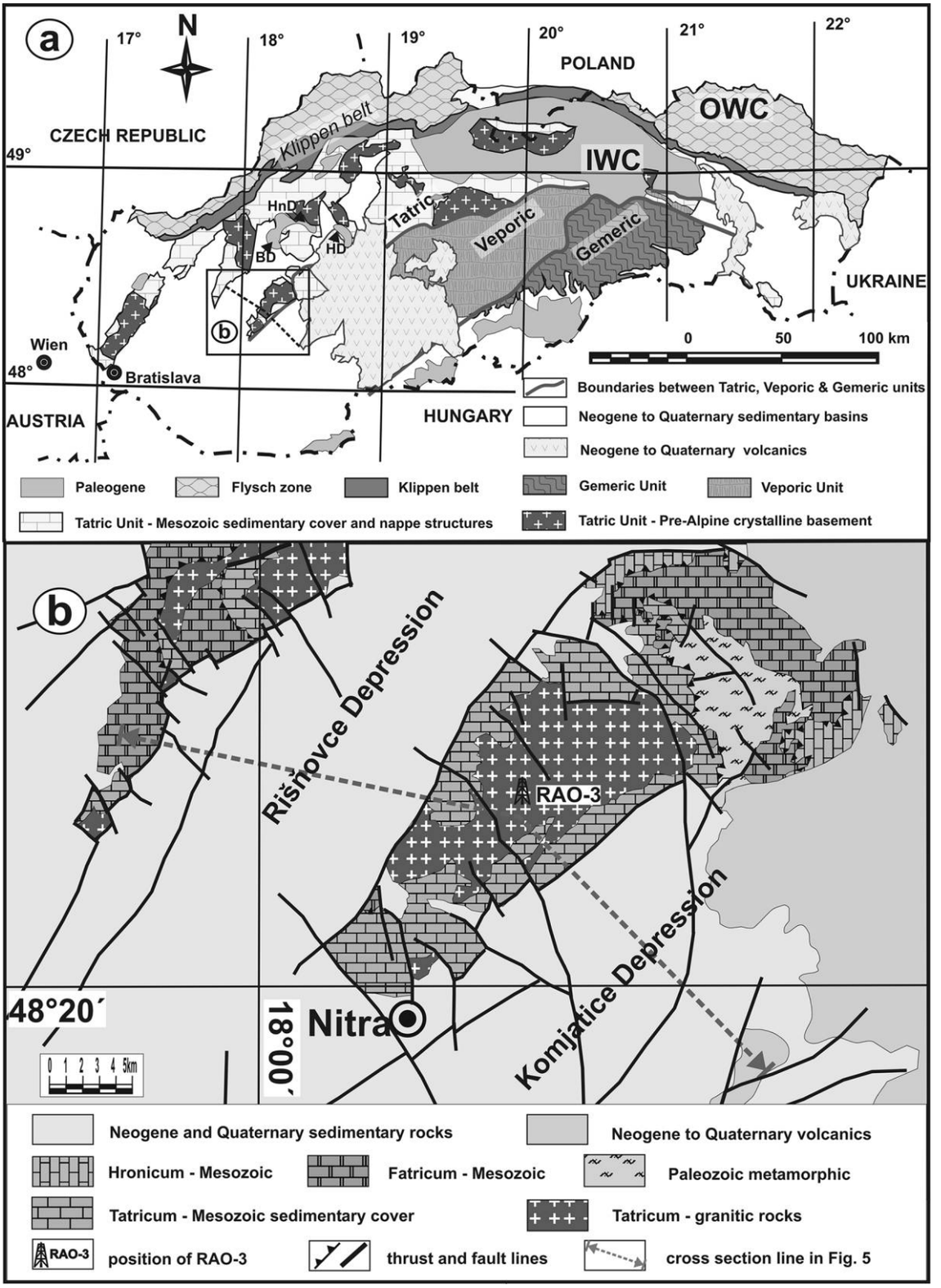

Figure 1. Simplified geological maps and positions of studied samples. *a*, Position of the Tribeč Mountains within the Western Carpathians in Slovakia. *b*, Simplified geological map of the Tribeč Mountains and their surroundings (modified after Elečko et al. 2008). BD = Bánovce Depression; HD = Handlová Depression; HnD = Horná Nitra Depression; IWC = Inner Western Carpathians; OWC = Outer Western Carpathians. A color version of this figure is available online.

These granitic rocks were recently dated by the secondary-ion mass spectrometry (SIMS) U-Pb zircon method to be ca. 368 ± 2.5 to 358 ± 2.9 Ma (Broska et al. 2013), and biotite $^{40}Ar/^{39}Ar$ step-heating ages demonstrated that the biotites had been thermally disturbed, with cooling ages between ca. 380 and 334 Ma (Kráľ et al. 2002). The studied pseudotachylytes form veins between 0.5 and 2.5 cm in thickness and branched dendritic injection veins of <0.5 cm in thickness. The pseudotachylytes are typically dark gray; the matrix comprises hematite (5%–45%), albite, and K-feldspar, whereas frequent host-rock clasts are formed by feldspars and quartz (fig. 2).

The Tribeč Mountains and neighboring intramontane depressions—Rišňovce and Komjatice—originated as a result of extensional tectonics during the Cenozoic in the IWC. The Miocene sediments of these two depressions overlie eroded and tectonically disrupted pre-Cenozoic substratum that has been drilled in several boreholes (fig. 5). It is noteworthy that there were no Paleogene sedimentary remnants identified in the vicinity of the Tribeč Mountains, and the nearest surface appearances of the Paleogene strata are ~20 km north from the Tribeč Mountains, in the Bánovce Depression (fig. 1*a*). Indeed, the Paleogene superficial occurrences are not extensive because of the Miocene cover. Up to 1300 m of the

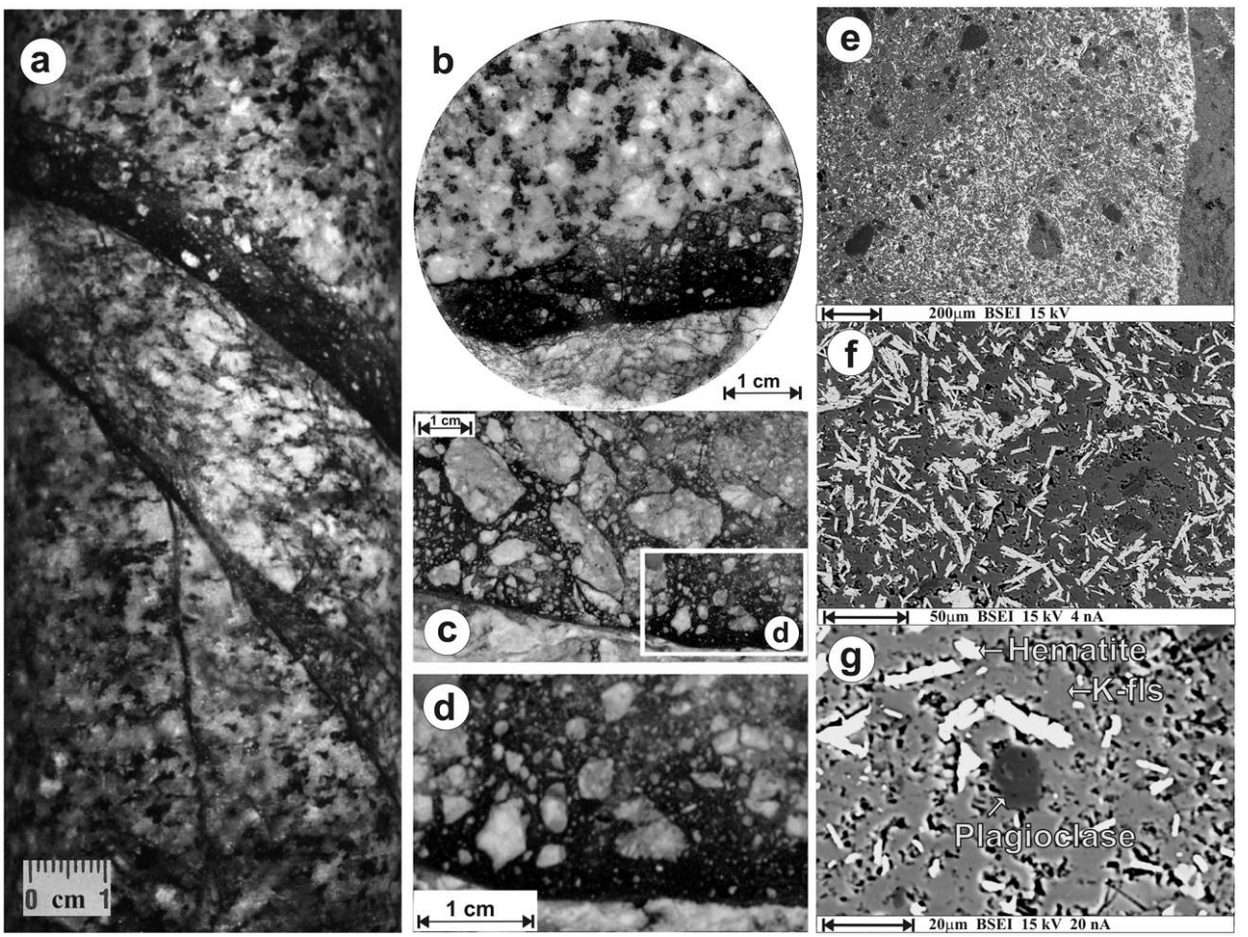

Figure 2. Photographs of typical structures and textures of the host granitic rocks and pseudotachylytes. *a*, Drill core from a deepness of 110.5 m.; tonalite sample with major pseudotachylyte and small injection veins (in natural size). *b*, Identical sample cross-cutting. *c*, Sample RAO-3/108 m with distribution of large host-rock porphyroclasts. *d*, Enlarged detail from *c*; sharp contact of pseudotachylyte dominated by dark aphanitic melt, with host-rock tonalite. *e*, Back-scattered electron (BSE) image showing distribution of microporphyroclasts in the pseudotachylyte melt. Sample RAO-3/110.5 m. *f*, BSE image showing dendritic texture, suggesting rapid crystallization from frictional melt. *g*, BSE image detail documenting intergrowth of principal mineral phases; view from identical sample RAO-3/110.5 m. K-fls = K-feldspar. A color version of this figure is available online.

Eocene (Bartonian to Priabonian) carbonaceous breccias and conglomerates, sandstones, bioclastic limestones, clays and claystones, and flysch sequences were drilled in borehole BnB-1, located in the center of a fault-bonded irregular structure, due to hydrothermal exploration, according to Gross in Elečko et al. (2008). The Lower Miocene (Eggenburgian to Karpatian) marine to brackish sedimentary fill and the Middle Miocene (Badenian to Sarmatian) brackish to limnic or lacustrine sediments of the Bánovce Depression reach up to 2500 m, whereas in the adjacent (southwest-continued) Rišňovce Depression these strata reach up to 3500 m in thickness (e.g., Biela 1978; fig. 5). The Neogene sediments of the Komjatice Depression have a stratigraphic range of the Middle Badenian (Middle Miocene) to Pliocene reaching up to 3000 m (Biela 1978). The sedimentary fill during the Miocene megacycle was characterized by a gradual decrease in salinity of the depositional environment. There are three lower-order shallowing-upward cycles in the sedimentary record, while the depositional environment changed from marine to brackish, brackish, and lacustrine swamp, with coal deposition in the northwestern margin of the Pannonian Basin. This succession is overlain by a Pliocene cycle composed of deltaic and fluvial deposits (Hók et al. 1999).

Analytical Methods

In situ laser microprobe $^{40}Ar/^{39}Ar$ spot analyses were performed at the Open University (Milton Keynes, United Kingdom) using a New Wave 213-nm UV laser coupled with a Nu Instruments Noblesse noble gas mass spectrometer. Pieces of polished thick sections (~300-μm thick) were cleaned in alternate methanol and deionized water prior to being packaged in aluminium foil. Samples were irradiated at McMaster (Canada) for 50 h, and neutron flux was monitored using biotite standard GA1550, with an age of 98.8 ± 0.5 Ma (Renne et al. 1998) and a calculated J value of 0.0121 ± 0.000064. All analyses were performed on areas of friction melt (pseudotachylyte), taking particular care to avoid entrained or refractory mineral clasts and to avoid regions at the vein margin that could be ultracataclasite rather than melt (e.g., Sherlock et al. 2009). Results were corrected for blanks on either side of two consecutive analyses, ^{37}Ar decay and neutron-induced interference reactions. The correction factors used were $(^{39}Ar/^{37}Ar)_{Ca} = 0.00065$, $(^{36}Ar/^{37}Ar)_{Ca} = 0.000264$, and $(^{40}Ar/^{39}Ar)_{K} = 0.0085$, based on analyses of Ca and K salts. See Sherlock and Hetzel (2001) for further details.

Results

One representative pseudotachylyte sample from a depth of 108 m (fig. 2*d*) was selected for laser microprobe $^{40}Ar/^{39}Ar$ analysis; data are presented in table 1. The 19 spot ages range from 79 ± 1 to 46 ± 1 Ma; excluding the oldest age, the weighted mean of the remaining 18 data points is 49.7 ± 1.3 Ma. Plotting the ages as a function of probability (fig. 3) identifies a common pattern of decreasing probability with age. There are two possible interpretations: (1) the incorporation of refractory host-rock minerals and clasts provide an older $^{40}Ar/^{39}Ar$ age component that is subordinate to the "pristine" melt component (e.g., Kohút and Sherlock 2003; Sherlock et al. 2004) or (2) the pseudotachylyte veins are partially overprinted by a subsequent thermal event, giving rise to a heterogeneous resetting of the vein material. Plotting $^{37}Ar_{Ca}/^{39}Ar_{K}$ versus age is used as one test for the possible incorporation of refractory clasts and host-rock pieces in a pseudotachylyte (e.g., Kohút and Sherlock 2003; Sherlock et al. 2009), but in this case the measured $^{37}Ar_{Ca}$ values are very low, indicating an overall Ca-poor pseudotachylyte. $^{38}Ar_{Cl}/^{39}Ar_{K}$ is more informative and indicates that the older ages correlate with higher $^{38}Ar_{Cl}/^{39}Ar_{K}$ ratios (fig. 4), which can be interpreted as the incorporation of refractory mineral pieces that have a precursor excess $^{40}Ar_{E}$ component trapped in fluid inclusions (e.g., Sherlock et al. 2009). The weighted mean age of 49.7 ± 1.3 Ma coincides with the highest probability age in figure 3. This pseudotachylyte-forming event is most likely connected to the Middle Paleogene–Eocene (ca. 49–46 Ma) seismic/tectonic events suggested for the southern part of the CCPB. However, we suppose propagation of the subvertical basement marginal faults during this time in the Tribeč Mountains to be a consequence of the continent-continent collision between the European and the Adriatic promontory as a result of the lateral extrusion model (Ratschbacher et al. 1989). These marginal faults facilitated subsequent unroofing of Tribeč Mountain basement during the Eocene-Miocene extensional and transpressional processes (fig. 5).

Discussion

The Western Carpathian pre-Cenozoic substratum in the Tatric Unit comprises pre-Mesozoic crystalline basement (dominated by Variscan granitic rocks and metamorphites, with scarce remnants of older metaigneous and metasedimentary rocks)—parautochthonous sedimentary units that represent the Mesozoic cover sequence, mainly carbonate

Table 1. $^{40}Ar/^{39}Ar$ Laser-Probe Data for the Pseudotachylytes

Analysis no.	^{40}Ar	^{39}Ar	^{38}Ar	^{37}Ar	^{36}Ar	$^{40}Ar^{*}/^{39}Ar$	Age
1	15,148.292 (±167.989)	2632.540 (±20.895)	34.714 (±2.518)	111.027 (±11.103)	.033 (±.119)	5.751 (±.080)	79.0 (±1.1)
2	7735.171 (±311.108)	2111.532 (±44.168)	24.119 (±1.103)	7.519 (±12.532)	.123 (±.108)	3.646 (±.167)	50.5 (±2.3)
3	3842.023 (±52.060)	1116.984 (±25.307)	12.220 (±.758)	10.030 (±220.667)	.196 (±.091)	3.388 (±.093)	47.0 (±1.3)
4	4136.530 (±19.757)	1233.782 (±9.029)	14.647 (±.669)	10.043 (±55.236)	.388 (±.190)	3.446 (±.054)	47.8 (±.8)
5	4926.578 (±26.294)	1385.551 (±10.059)	15.548 (±.759)	221.170 (±5.027)	.076 (±.099)	3.539 (±.038)	49.1 (±.6)
6	2927.688 (±14.024)	856.103 (±12.422)	9.623 (±.521)	276.565 (±15.085)	.060 (±.088)	3.441 (±.061)	47.7 (±.9)
7	6134.755 (±164.964)	1841.523 (±27.610)	18.881 (±.910)	173.584 (±22.641)	.057 (±.139)	3.340 (±.105)	46.3 (±1.5)
8	3544.322 (±156.088)	786.745 (±16.971)	9.947 (±1.226)	226.532 (±110.749)	.339 (±.278)	4.378 (±.243)	60.5 (±3.3)
9	6256.756 (±44.359)	1629.985 (±20.717)	19.170 (±1.364)	211.798 (±15.128)	.087 (±.320)	3.854 (±.081)	53.4 (±1.1)
10	12,492.558 (±470.951)	3367.904 (±81.483)	39.018 (±1.587)	225.034 (±281.292)	.038 (±.153)	3.706 (±.167)	51.3 (±2.3)
11	19,260.624 (±557.175)	5534.804 (±51.684)	63.724 (±1.904)	17.919 (±58.875)	.085 (±.072)	3.484 (±.106)	48.3 (±1.5)
12	18,531.879 (±327.125)	5240.887 (±18.250)	61.297 (±1.830)	957.917 (±215.147)	.216 (±.105)	3.548 (±.064)	49.2 (±.9)
13	23,186.107 (±74.921)	6849.430 (±37.747)	79.677 (±2.181)	584.347 (±35.881)	.167 (±.061)	3.392 (±.022)	47.0 (±.4)
14	15,300.797 (±172.424)	4134.695 (±66.595)	52.760 (±2.951)	1323.268 (±15.387)	.315 (±.135)	3.723 (±.074)	51.6 (±1.0)
15	14,557.360 (±30.068)	3803.193 (±13.377)	42.436 (±.991)	38.493 (±7.699)	.147 (±.070)	3.816 (±.016)	52.8 (±.3)
16	20,616.544 (±124.405)	5696.613 (±47.086)	64.169 (±1.673)	182.277 (±156.605)	.151 (±.090)	3.611 (±.037)	50.0 (±.6)
17	15,472.963 (±511.086)	3914.675 (±95.226)	46.219 (±1.734)	38.024 (±66.419)	.285 (±.089)	3.931 (±.162)	54.4 (±2.2)
18	9052.087 (±89.039)	2148.224 (±41.114)	31.026 (±2.154)	119.065 (±91.375)	.018 (±.068)	4.211 (±.091)	58.2 (±1.3)
19	11,316.934 (±18.635)	3207.108 (±26.929)	34.714 (±1.166)	83.117 (±38.788)	.052 (±.106)	3.533 (±.032)	49.0 (±.5)

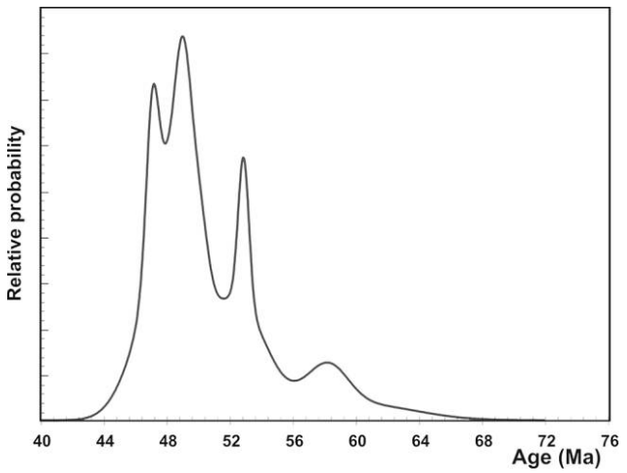

Figure 3. Cumulative probability plot for analyzed pseudotachylyte ages constructed using Isoplot (Ludwig 1999). The pseudotachylyte age is best explained by the main peak, whereas the incorporation of refractory host-rock minerals and clasts have provided older ages. A color version of this figure is available online.

lithologies that are Lower Triassic to Albian in age. The Upper Mesozoic nappe structure is represented by the Fatricum and Hronicum nappes. Fatricum is generally built by similar Triassic to Cretaceous carbonate lithologies comparable to the cover sequence, with a minor contribution from clastics, and have comparable stratigraphic span (Lower Triassic to the Albian), whereas pre-Alpine basement fragments are present only locally (Hók et al. 1994; Froitzheim et al. 2008). Hronicum is the uppermost large cover nappe system, and at its base it has a thick pile of Late Paleozoic volcanics and clastics, followed by a huge Triassic carbonate succession and scattered Jurassic and Lower Cretaceous remnants. It is noteworthy that the Mesozoic rock successions do not exceed 4.5–5 km in thickness, including local internal imbrications. However, the Gosau Upper Cretaceous (postnappe stacking sedimentary sequence) has not been identified near the study area, and because the Gosau posttectonics sediments are only known close to the Klippen Belt in the IWC, we suggest that the 4.5–5-km Mesozoic rock pile is the maximum that could have covered crystalline basement in the Tribeč Mountains before sedimentation of the Paleogene strata. There was a long period (~30 m.yr.) from the Coniacian to the Ypresian before a new period of sedimentation began within the CCPB; on the other hand, we cannot exclude potential continental sedimentation that was eroded later in the study area. During Paleogene times, the CCPB developed on the northern edge of the ALCAPA plate as a forearc basin. Generally, sedimentation in the CCPB began by shallow-water transgressive coarse-grained clastics during the Ypresian (57–55 Ma; Gross et al. 1984), derived mainly from the base Hronicum carbonates, and these breccias, conglomerates, and sandstones are mainly found near the Klippen Belt (fig. 1*a*) at present day. The Paleogene sedimentation around the Tribeč Mountains (southern branch of the CCPB, according Chmelík in Buday et al. 1967) started ~10 m.yr. later, in the Lutetian, similarly over the Hronicum base, from which coarse-grained clastics were also derived. The maximum thickness of the Paleogene sediments beneath the Miocene strata in the Bánovce Depression and neighboring the Horná Nitra Depression and the Handlová Depression do not exceed 1500 m today. Interestingly, the first Paleogene conglomerates containing pebbles and boulders from the surrounding crystalline basement appeared in the Horná Nitra Depression and the Handlová Depression at the Bartonian-Priabonian boundary (ca. 37 Ma) as intraformation breccias, the Podremata conglomerates (Zlinská and Gross 2013). Although Danišík et al. (2004) suggest that the Tribeč Mountains were uplifting during the Eocene and massive contemporaneous sedimentary records in the Bánovce Depression, the Horná Nitra Depression, and the Handlová Depression indicate progressive subsidence in neighboring areas, we cannot exclude possible Lower Eocene sedimentation over the Tribeč Mountains before their uplift. However, variegated georelief must have already existed in the Paleogene, and depositional basins were separated from exhumed denudation planation surfaces by normal faults at the beginning of the Eocene-Miocene extensional exhumation tectonics in the IWC.

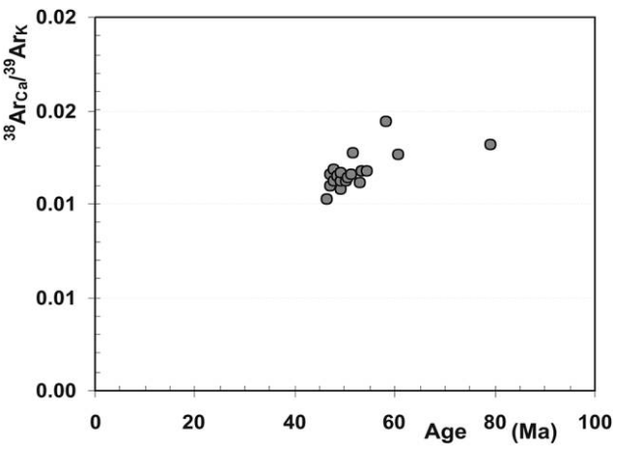

Figure 4. $^{38}Ar_{Cl}/^{39}Ar_K$ versus age for pseudotachylytes. The uncertainties are smaller than the sizes of the ornament used on the plot. A color version of this figure is available online.

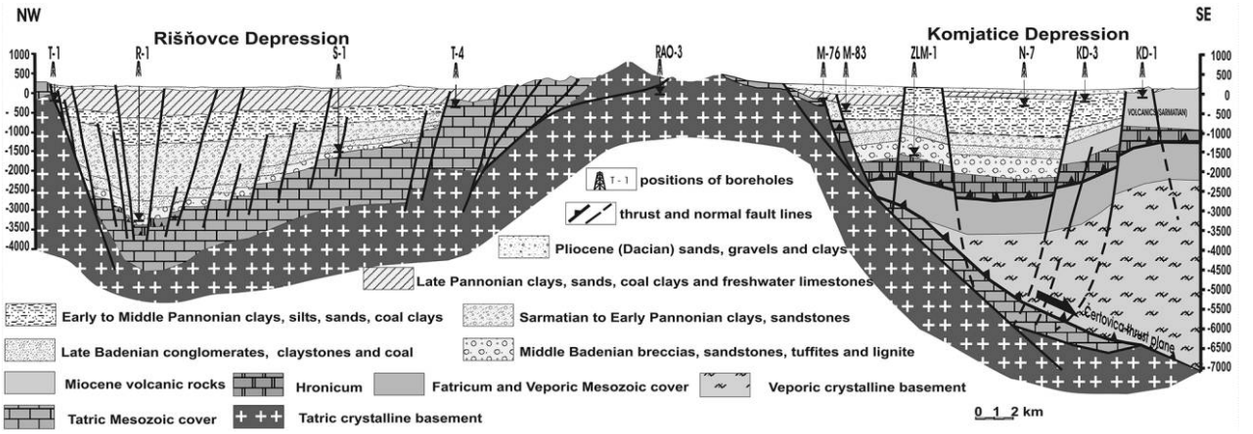

Figure 5. Geological cross section of the studied area. The situation in the Rišnovce Depression is modified from Elečko et al. (2008), and that in the Komjatice Depression is modified from Hók et al. (1999). A color version of this figure is available online.

Quantifying the integrated erosion and sink processes raises the question of how deep the pseudotachylytes formed in the studied area. Pseudotachylytes are produced at shallow (2–10 km) and midcrustal (10–20 km) levels (Di Toro et al. 2009 and citations therein) as a consequence of the intermediate and deep earthquakes from greater depth. Field and theoretical studies as well as petrological and structural studies demonstrate that the pseudotachylytes were generated by relatively high-stress seismic faulting in crystalline sialic crust at a depth of ~4–5 km (Sibson 1975; Toyoshima 1990) linked to brittle regimes. Other pseudotachylytes are closely linked to plastic-ductile regimes associated with greenschist, amphibolite, and/or granulitic facies mylonites (Sibson 1980; Passchier 1982; Clarke and Norman 1993; White 1996). When trying to constrain the depth of pseudotachylyte formation, it is necessary to take into account the eroded rock pile: ~0.5–1 km of the eroded crystalline basement, 4.5–5 km of the Mesozoic cover and nappe sediment sequences, and 0.5–1 km of the Paleogene uncertain sediments. This implies that Tribeč Mountain pseudotachylytes were derived at depths of no more than 5.5 to 7 km. This is a minimum estimate for the depth of their burial and their present position, close to the surface, and it suggests the magnitude of their exhumation.

While the pseudotachylyte $^{40}Ar/^{39}Ar$ age dating presented here is new in the Tribeč Mountains, the earlier Alpine tectonic deformation of the Tribeč Mountain granitic rocks has been documented on white micas from shear zone mylonites, with $^{40}Ar/^{39}Ar$ staircase spectra indicating that mylonitization occurred before ca. 71–63 Ma (Kráľ et al. 2002). Additional Tribeč Mountain thermochronological data can be found in the work of Kováč et al. (1994), who presented one zircon fission track (ZFT) age of 53 ± 12 Ma and one apatite fission track (AFT) age

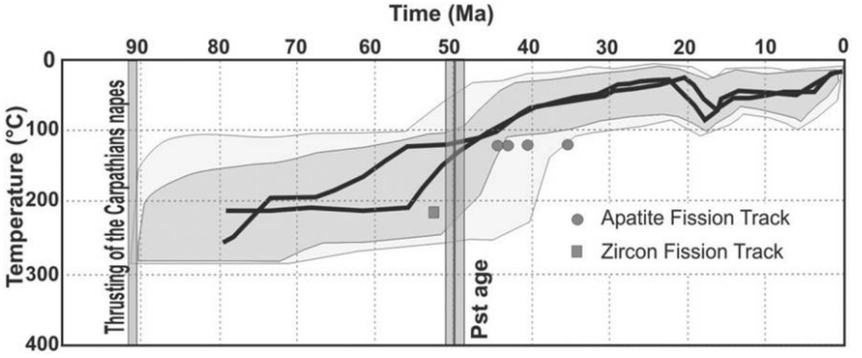

Figure 6. Thermal history of the Tribeč Mountain pseudotachylytes. The time-temperature path is derived from zircon fission track (Kováč et al. 1994) and apatite fission track (Danišík et al. 2004) analysis. Thermal modeling results of apatite fission track analysis are taken from Danišík et al. (2004). Pst = pseudotachylyte. A color version of this figure is available online.

of 28 ± 1 Ma determined using an old population method (POP), whereas Danišík et al. (2004) reported four AFT ages from the Tribeč Mountain crystalline basement ranging from 43.7 ± 2.9 to 34.8 ± 1.9 Ma determined using a modern external detector method. These data suggest that Tribeč Mountain pseudotachylytes originated between 53 ± 12 and 43.7 ± 2.9 Ma in host-rock granodiorites between 210°C and ~110°C and/or indicate a significant and widespread Eocene exhumation event (fig. 6). It is notable that our previous pseudotachylyte dating from the Tatra Mountains (Kohút and Sherlock 2003) yield similar ages varying between 58 and 31 Ma, with a weighted mean of 43.6 ± 1.4 Ma. However, thermochronological dating has yielded other results for the surrounding Tatra Mountain granodiorites: ZFT ages varying from 73.1 to 62.6 Ma (Králiková 2013), zircon U-Th/He (ZHe) ages varying from 45 to 40 Ma (Śmigielski et al. 2012), and AFT ages varying from 20.3 to 9.3 Ma (Śmigielski et al. 2012; Králiková 2013). There is good correlation with the model of Kirpatrick et al. (2012) in low-temperature geochronology, where the timing of pseudotachylyte formation was the same as the ZHe age. Assuming a geothermal gradient of 30°C/km and ZHe closure temperatures of ~190° ± 10°C (Reiners et al. 2004) implies that the Tatra Mountain pseudotachylytes might have formed at a similar depth of ~6 km. It is apparent that both occurrences of well-documented pseudotachylytes in the IWC originated from seismic activity following a period of quiescence in the sedimentary record and mirrored inception phases of the Paleogene extensional tectonics in the Western Carpathians.

Conclusions

Taking into account the recent geological situation, the Paleogene and Neogene sedimentation, modern ZFT and AFT data, and our pseudotachylyte dating, we can conclude the following.

1. The study area is part of the CCPB. Its sedimentation began at the Paleocene-Eocene boundary (proximal-northern part near the Klippen Belt in Ypresian) or at the Eocene Bartonian-Priabonian boundary (southern part of the CCPB surrounding the Tribeč Mountains, e.g., the Bánovce Depression, the Horná Nitra Depression, and the Handlová Depression).

2. The maximal burial of the southern part of the CCPB (surrounding the Tribeč Mountains) is likely to have occurred ca. 50–46 Ma, although the sedimentary record is missing in neighboring intramontane basins—the Rišňovce and Komjatice Depressions.

3. The seismogenic pseudotachylytes document tectonic activity from the Tribeč Mountains (weighted mean age: 49.7 ± 1.3 Ma) and indicate the beginning of the Eocene exhumation due to extensional tectonics of the broad southern part of the CCPB rather than prolonged progressive burial, given the general absence of Paleogene sediments in surrounding areas.

4. During the Miocene, the Tribeč Mountain crystalline basement progressively eroded, and the neighboring Neogene Rišňovce and Komjatice Depressions at the northwestern margin of the Pannonian Basin were filled by contemporaneous strata.

ACKNOWLEDGMENTS

This work was supported by the Slovak Research and Development Agency under contract APVV 0549-07 to M. Kohút. S. C. Sherlock gratefully acknowledges support from Natural Environment Research Council (NERC) grant NER/F020066/1. The manuscript benefited from constructive reviews by J. Hók (Comenius University, Bratislava, Slovakia) and D. B. Rowley (University of Chicago), which is greatly appreciated. We thank D. B. Rowley for editorial handling and suggested improvements to the manuscript.

REFERENCES CITED

Andrusov, D. 1968. Grundriss der Tektonik der nördlichen Karpaten. Bratislava, Veda, 188 p.

Biela, A. 1978. Deep drillings in the covered areas of the Inner Western Carpathians. Regionálna geológia Západných Karpát 10, 224 p. (in Slovak).

Broska, I.; Petrík, I.; Shlevin, Y. B.; Majka J.; and Bezák, V. 2013. Devonian/Mississippian I-type granitoids in the Western Carpathians: a subduction-related hybrid magmatism. Lithos 162:27–36.

Buday, T.; Cícha, I.; Hanzlíková, E.; Chmelík, F.; Koráb, T.; Kuthan, M.; Nemčok, J.; et al. 1967. Regional geology of Czechoslovakia—part II. Western Carpathian Mountains. Prague, Academia Praha, 723 p.

Clarke, G. L., and Norman, A. R. 1993. Generation of pseudotachylite under granulite facies conditions, and its preservation during cooling. J. Met. Geol. 11:319–335.

Csontos, L.; Nagymarosy, A.; Horváth, F.; and Kováč, M. 1992. Tertiary evolution of the intracarpathian area: a model. Tectonophysics 208:221–241.

Danišík, M.; Dunkl, I.; Putiš, M.; Frisch, W.; and Kráľ, J. 2004. Tertiary burial and exhumation history of basement highs along the NW margin of the Pannonian

Basin—an apatite fission track study. Austrian J. Earth Sci. 95/96:60–70.
Danišík, M.; Kadlec, J.; Glotzbach, C.; Weisheit, A.; Dunkl, I.; Kohút, M.; Orvošová, M.; and Evans, N. J. 2011. Tracing metamorphism, exhumation and topographic evolution in orogenic belts by multiple thermochronology: a case study from the Nízke Tatry Mts., Western Carpathians. Swiss J. Geosci. 104:285–298.
Danišík, M.; Kohút, M.; Broska, I.; and Frisch, W. 2010. Thermal evolution of the Malá Fatra Mountains (Central Western Carpathians): insights from zircon and apatite fission track thermochronology. Geol. Carpathica 61:19–27.
Danišík, M.; Kohút, M.; Dunkl, I.; and Frisch, W. 2008. Thermal evolution of the Žiar Mountains basement (Inner Western Carpathians, Slovakia) constrained by fission track data. Geol. Carpathica 59:19–30.
Di Toro, G.; Pennacchioni, G.; and Nielsen, S. 2009. Pseudotachylytes and earthquake source mechanics. Int. Geophys. 94:87–133.
Elečko, M.; Maglay, J.; Pristaš, J.; Fordinál, K.; Nagy, A.; Konečný, V.; Šimon, L.; et al. 2008. General geological map of the Slovak Republic, scale 1 : 200,000, sheet 35, Trnava, Dionýz Štúr State Institute of Geology.
England, P., and Molnar, P. 1990. Surface uplift, uplift of rocks, and exhumation of rocks. Geology 18:1173–1177.
Froitzheim, N.; Plašienka, D.; and Schuster, R. 2008. Alpine tectonics of the Alps and Western Carpathians. *In* McCann, T., ed. The geology of Central Europe. London, Geological Society, p. 1141–1232.
Gross, P.; Köhler, E.; and Samuel, O. 1984. A new lithostratigraphic division of the Inner-Carpathian Paleogene. Geol. Práce Správy 81:103–117 (in Slovak with English summary).
Hók, J.; Ivanička, J.; and Kováčik, M. 1994. Geological structure of the Rázdiel part of the Tríbeč Mts., Western Carpathians: new knowledge and discussion. Mineral. Slovaca 26:192–196 (in Slovak with English summary).
Hók, J.; Kováč, M.; Kováč, P.; Nagy, A.; and Šujan, M. 1999. Tectonic and geological evolution of the NE part of the Komjatice Depression. Slovak Geol. Mag. 5:187–199.
Kázmér, M.; Dunkl, I.; Frisch, W.; Kuhlemann, J.; and Ozsvárt, P. 2003. The Palaeogene forearc basin of the Eastern Alps and the Western Carpathians: subduction erosion and basin evolution. J. Geol. Soc. Lond. 160:413–428.
Kirkpatrick, J. D.; Dobson, K. J.; Mark, D. F.; Shipton, Z. K.; Brodsky, E. E.; and Stuart, F. M. 2012. The depth of pseudotachylyte formation from detailed thermochronology and constraints on coseismic stress drop variability. J. Geoph. Res. 117:B06406.
Kohút, M., and Sherlock, S. C. 2003. Laser microprobe ^{40}Ar-^{39}Ar analysis of pseudotachylyte and host rocks from the Tatra Mountains, Slovakia: evidence for Late Paleogene seismic/tectonic activity. Terra Nova 15: 417–424.
Kováč, M. 2000. Geodynamic, paleogeographic and structural evolution of the Carpathian-Pannonian region during the Miocene: new overview to the Neogene basins of Slovakia. Bratislava, Veda, 202 p. (in Slovak with English summary).
Kováč, M.; Kráľ, J.; Márton, E.; Plašienka, D.; and Uher, P. 1994. Alpine uplift history of the Central Western Carpathians: geochronological, paleomagnetic, sedimentary and structural data. Geol. Carpathica 45:83–96.
Kráľ, J.; Hók, J.; Frank, W.; Siman, P.; Liščák, P.; and Jánová, V. 2002. Shear deformation in granodiorite: structural, ^{40}Ar/^{39}Ar, and geotechnical data (Tribeč Mts., Western Carpathians). Slovak Geol. Mag. 8:235–246.
Králiková, S. 2013. Low-thermal evolution of the Central Western Carpathian rock complexes during the Alpine tectogenesis. PhD thesis, Comenius University, Bratislava.
Ludwig, K. 1999. Isoplot/Ex. 2.01: a geochronological toolkit for Microsoft Excel. Berkeley, CA, Berkeley Geochronological Center.
Madarás, J.; Kohút, M.; Ivanička, J.; Marsina, K.; and Kováčik, M. 2004. Geological interpretation of the structural borehole RAO-3 (Tribeč Mts.). Geol. Práce 109:41–49 (in Slovak with English summary).
Maghlouglin, J. F., and Spray, J. G. 1992. Frictional melting processes and products in geological materials: introduction and discussion. Tectonophysics 204:197–204.
Minár, J.; Bielik, M.; Kováč, M.; Plašienka, D.; Barka, I.; Stankoviansky, M.; and Zeyen, H. 2011. New morphostructural subdivision of the Western Carpathians: an approach integrating geodynamics into targeted morphometric analysis. Tectonophysics 502:158–174.
Passchier, C. W. 1982. Pseudotachylyte and the development of ultramylonite bands in the Saint-Barthelémy Massif, French Pyrenees. J. Struct. Geol. 4:69–79.
Philpotts, A. R. 1964. Origin of pseudotachylites. Am. J. Sci. 262:1008–1035.
Plašienka, D. 1999. Tectochronology and paleotectonic model of Jurassic-Cretaceous evolution of Central Western Carpathians. Bratislava, Veda, 125 p. (in Slovak with English summary).
Ratschbacher, L.; Frisch, W.; Neubauer, F.; Schmid, S. M.; and Neugebauer, J. 1989. Extension in compressional orogenic belts: the eastern Alps. Geology 17:404–407.
Reimold, W. U. 1995. Pseudotachylite in impact structures—generation by friction melting and shock brecciation? a review and discussion. Earth-Sci. Rev. 39: 247–265.
Reimold, W. U.; Jessberger, E. K.; and Stephan, T. 1990. ^{40}Ar/^{39}Ar dating of pseudotachylite from the Vredefort Dome, South Africa: a progress report. Tectonophysics 171:139–152.
Reiners, P. W., and Brandon, M. T. 2006. Using thermochronology to understand orogenic erosion. Ann. Rev. Earth Planet. Sci. 34:419–466.
Reiners, P. W.; Spell, T. L.; Nicolescu, S.; and Zanetti, K. A. 2004. Zircon (U-Th)/He thermochronometry: He diffusion and comparisons with ^{40}Ar/^{39}Ar dating. Geochim. Cosmochim. Acta 68:1857–1887.
Renne, P. R.; Swisher, C. C.; Deino, A. L.; Karner, D. B.; Owens, T. L.; and DePaolo, D. J. 1998. Intercalibration

of standards, absolute ages and uncertainties in Ar/Ar dating. Chem. Geol. 145:117–152.
Ring, U.; Brandon, M. T.; Willett, S. D.; and Lister, G. S. 1999. Exhumation processes. *In* Ring, U.; Brandon, M. T.; Lister, G. S.; and Willett S., eds. Exhumation processes: normal faulting, ductile flow and erosion. Geol. Soc. Lond. Spec. Publ. 154:1–27.
Sherlock, S. C., and Hetzel, R. 2001. A laser-probe $^{40}Ar/^{39}Ar$ study of pseudotachylite from the Tambach Fault Zone, Kenya: direct isotopic dating of brittle faults. J. Struct. Geol. 23:33–44.
Sherlock, S. C.; Jones, K. A.; and Park, R. G. 2008. Grenville-age pseudotachylite in the Lewisian: laser-probe $^{40}Ar/^{39}Ar$ ages. J. Geol. Soc. Lond. 165:73–83.
Sherlock, S. C.; Strachan, R. A.; and Jones, K. A. 2009. High spatial resolution $^{40}Ar/^{39}Ar$ dating of pseudotachylites: geochronological evidence for multiple phases of faulting within basement gneisses of the Outer Hebrides (UK). J. Geol. Soc. Lond. 166:1049–1059.
Sherlock, S. C.; Watts, L. M.; Holdsworth, R. E.; and Roberts, D. 2004. Dating fault reactivation by Ar/Ar laserprobe: an example from the Møre-Trøndelag Fault Complex. J. Geol. Soc. Lond. 161:335–358.
Sibson, R. H. 1975. Generation of pseudotachylite by ancient seismic faulting. Geophys. J. R. Astron. Soc. 43:775–794.
———. 1980. Transient discontinuities in ductile shear zones. J. Struct. Geol. 2:165–171.
Śmigielski, M.; Stuart, F. M.; Krzywiec, P.; Persano, C.; Sinclair, H. D.; Pisaniec, K.; and Sobien, K. 2012. Neogene exhumation of the Northern Carpathians revealed by low temperature thermochronology. Geoph. Res. Abst. 14:EGU2012-12063.
Toyoshima, T. 1990. Pseudotachylite from the main zone of the Hidaka metamorphic belt, Hokkaido, northern Japan. J. Metamorph. Geol. 8:507–523.
Wagner, G. A., and Van den Haute, P. 1992. Fission-track dating. Stuttgart, Enke, 285 p.
White, J. C. 1996. Transient discontinuities revisited: pseudotachylyte, plastic instability and the influence of low pore fluid pressure on the deformation processes in the mid-crust. J. Struct. Geol. 18:1471–1486.
Zlinská, A., and Gross, P. 2013. Age and lithology determination in the Handlovska kotlina Basin Palaeogene deposits, based on the FGHn-1 (Handlova) well reinterpretation. Acta Geol. Slov. 5:141–153 (in Slovak with English summary).